ACTA PHYSICA POLONICA Vol. XXXV (1969) Fasc. 5

DEPENDENCE OF DOMAIN WIDTH ON CRYSTAL THICKNESS IN Fe—Si SINGLE CRYSTALS

By B. Wysłocki

Institute of Ferrous Metallurgy, Gliwice*

(Received July 30, 1968)

The dependence of the domain width D on the crystal thickness T in wedge-shaped single-crystalline Fe—Si samples is studied experimentally for the standard (*SL*) and modified (*ML*) Landau-Lifshitz domain structure, in the thickness range 20 μm $\lesssim T \lesssim$ 5 mm. Similarly as in uniaxial Co (Wysłocki 1968), the thickness dependence is found to be of the form $D_{X;m} = a_{X;m} T^{b_m}$ where $m = 1$, $b_1 = 0.5$ for $T \leqslant T_0$ and $m = 2$, $b_2 = 0.9$ for $T \geqslant T_0$. The subscript X denotes the type of domain structure ($X = SL$ or ML). The critical thickness T_0 is determined experimentally ($T_0 \cong 400$ μm for Fe—3.25% Si) and, for the *ML* domain structure, shown to correspond to an energy discontinuity. In the case of the *SL* domain structure, the failure of the standard Landau-Lifshitz theory is pointed out.

1. Introduction

In [1], the influence of the crystal thickness on the regular remanent domain structures in Co has been studied experimentally on a wedge-shaped single-crystalline sample, and the domain width D was found to depend on the crystal thickness T according to the formula

$$D = aT^b \tag{1}$$

where the exponent b assumes two different values, b_1 and b_2, for crystal thicknesses T below and above the critical thickness T_0 at which the dagger-like closure domains disappear[1]. The coefficient a in (1) depends on the type of the domain structure and differs for $T \leqslant T_0$ and $T \geqslant T_0$. By introducing the subscript X for the type of domain structure and the index m assuming the values 1 and 2 for $T \leqslant T_0$ and $T \geqslant T_0$, respectively, we can rewrite (1) in the form

$$D_{X;m} = a_{X;m} T^{b_m}, \quad m = \begin{cases} 1 & \text{for} \quad T \leqslant T_0 \\ 2 & \text{for} \quad T \geqslant T_0. \end{cases} \tag{2}$$

* Address: Zakład Materiałów Magnetycznych, Instytut Metalurgii Żelaza, Gliwice, Miarki 12, Polska.

[1] Note that in the present notation T_0 corresponds to T_1 in [1, 2] and shall not be confused with T_0 and T'_0 in those papers.

Two regular domain structures were examined in [1], namely, the honeycomb (H) and Goodenough (G) domain structure, and in either case the values of T_0, b_1, and b_2 were the same, *i.e.*, $T_0 \cong 50\ \mu\text{m} \equiv T_0^{Co}$, $b_1 = 0.5$ and $b_2 = 0.57$. The coefficients $a_{X;m}$ were found to satisfy the rules[2]

$$a_{H;1}/a_{H;2} \cong a_{G;1}/a_{G;2} \cong 1.3\ \mu\text{m}^{0.07} = 0.68\ \text{cm}^{0.07},$$

$$a_{H;1}/a_{G;1} \cong a_{H;2}/a_{G;2} \cong 1.5. \tag{3}$$

The results obtained in [1] on a wedge-shaped sample were fully confirmed in [2] (see also [3]) by analogous experiments carried through on a series of 15 rectangular-prism-shaped single crystals, their thicknesses in the magnetically easiest direction [0001] ranging from 3 μm to 11.5 mm. This led us to conclude that the general formula (2) may well be applicable to any (regular) domain structure in any ferromagnetic crystal, the exponent b_1 (for $T \leqslant T_0$) depending neither on the domain structure nor on the material, the critical thickness T_0 and the exponent b_2 depending on the material but not on the domain structure, and the coefficients $a_{X;m}$ depending on both the domain structure and the material. Furthermore, the relationships (3) seem to indicate the existence of the general rules

$$a_{X;1}/a_{X;2} = \underset{(X)}{\text{const}},\quad a_{X;m}/a_{Y;m} = \underset{(m)}{\text{const}'} \tag{4}$$

where the values of the constants depend on the material and X and Y correspond to two different regular domain structures that can form in the material (which actually depends on the number of magnetically preferred directions in the material).

The purpose of the present paper is in verifying this supposition by determining experimentally the thickness dependence of the domain width for two different regular domain structures in Fe-3.25%Si wedge-shaped single crystals, over a thickness range from 20 μm to 5 mm. The only earlier measurements of that type known to the author are those reported in [4–6], and these are far too inaccurate to suit our purpose.

2. *Observations and measurements*

Two wedge-shaped Fe-3.25% Si single crystals were used in our experiment, their dimensions and crystallographic orientations being as shown in Figs 1 and 2. The single crystals were grown from polycrystalline sheet iron by secondary recrystallization with temperature gradient shifting (see [7, 8]). The preparation of the samples (mechanical and electrolytical polishing, determination of crystallographic orientation, *etc.*) and the colloid used for the powder-pattern observations were as usual (see, *e.g.*, [4,9–13]). Observations of the domain structures and measurements of the domain widths (taken from enlarged photographs of the powder patterns) were performed on both the lateral faces of the wedge-shaped

[2] Note that for $T \leqslant T_0$ (*i.e.*, $m = 1$) and $T \geqslant T_0$ (*i.e.*, $m = 2$) the dimension of the coefficient $a_{X;m}$ is not the same if $b_1 \neq b_2$, as $[a_{X;1}] = [T]^{1-b_1}$ and $[a_{X;2}] = [T]^{1-b_2}$. Hence, $[a_{X;1}/a_{X;2}] = [T]^{b_2-b_1}$. In converting the results of [1, 2] from μm to cm note that $b_2 - b_1 = 0.07$, $1 - b_2 = 0.43$ for Co and $1\ \mu\text{m}^{0.07} = 0.525\ \text{cm}^{0.07}$, $1\ \mu\text{m}^{0.43} = 0.019\ \text{cm}^{0.43}$.

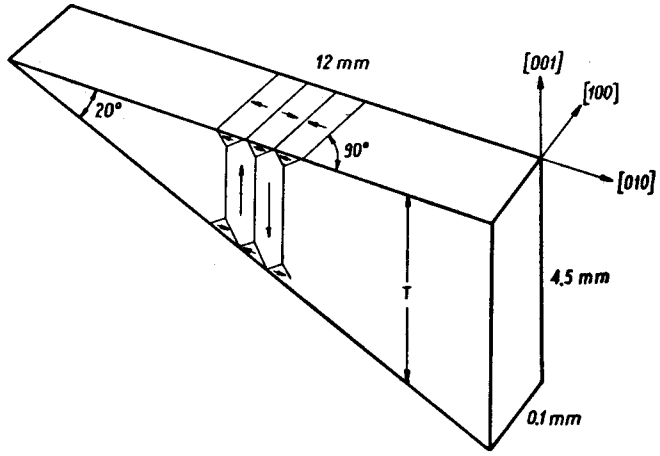

Fig. 1. Wedge-shaped Fe-3.25% Si single crystal with standard Landau-Lifshitz (*SL*) domain structure (*cp.* Figs 3 and 4)

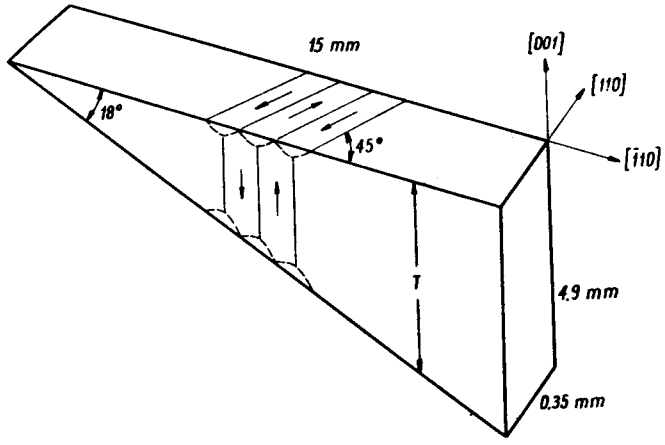

Fig. 2. Wedge-shaped Fe-3.25% Si single crystal with modified Landau-Lifshitz (*ML*) domain structure (*cp.* Figs 5, 8, 9)

samples and checked against those obtained on the upper crystal surfaces (001). To test the reliability of the measurements, each domain structure had been destroyed (by heating the crystals above the Curie temperature) and reproduced several times and the measurements repeated. This procedure served also as a precaution against incidental irregularities in the domain structures. In this way, quite satisfactory precision in measuring the domain width D and the crystal thickness T was achieved, the accuracy being ± 0.1 μm for small, and ± 5 μm for large D and T.

As expected, the domain structure of the sample from Fig. 1 was of the standard Landau--Lifshitz (*SL*) type [14], a model of which is shown in Fig. 3. Typical powder patterns from the lateral crystal surface (100) are presented in Fig. 4.

ACTA PHYSICA POLONICA Vol. XXXV (1969) Fasc. 5

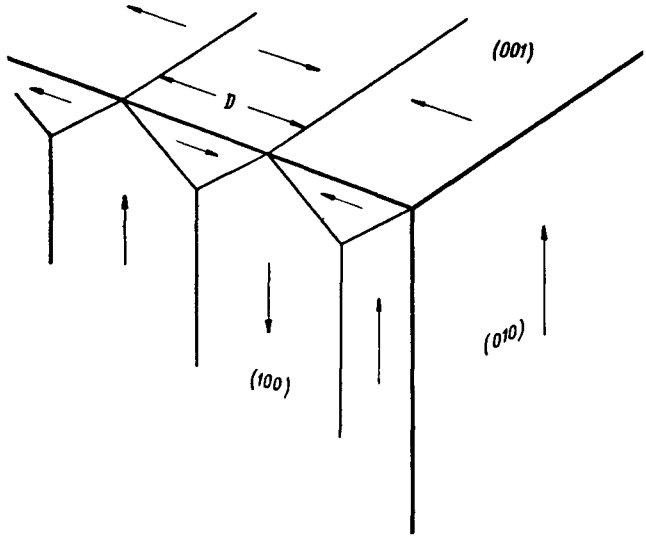

Fig. 3. Model of the standard Landau-Lifshitz (*SL*) domain structure (*cp.* Figs 1 and 4)

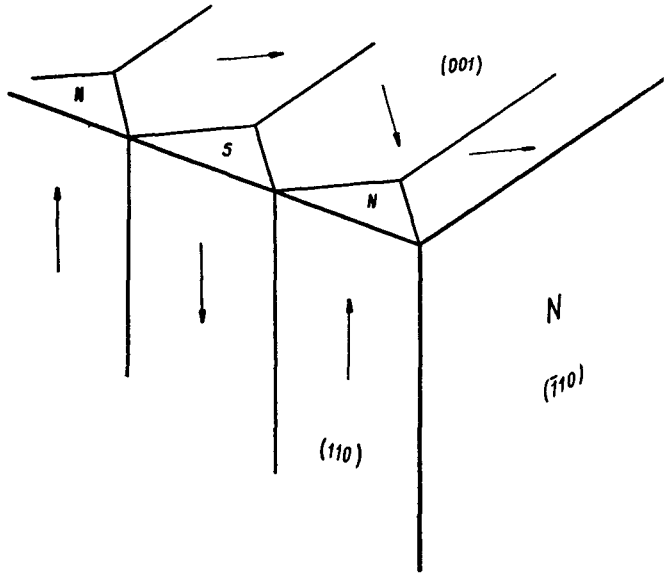

Fig. 6. Model of the Néel domain structure

A new type of domain structure has been observed in the sample from Fig. 2. As seen from the powder patterns reproduced in Fig. 5*a–c*, the 180° Bloch walls between the main domains inside the crystal form an angle of 45° with the lateral crystal surfaces (110), and the primary closure domains at the crystal surface (001) are magnetized parallel to the Bloch lines on this surface. The domain structure is therefore neither of the Néel type shown schematically in Fig. 6 nor of the standard Landau–Lifshitz type shown in Fig. 7, though either one can in principle exist in a crystal with faces as in Figs 6 and 7. The only reasonable

ACTA PHYSICA POLONICA Vol. XXXV (1969) Fasc. 5

ACTA PHYSICA POLONICA Vol. XXXV (1969) Fasc. 5

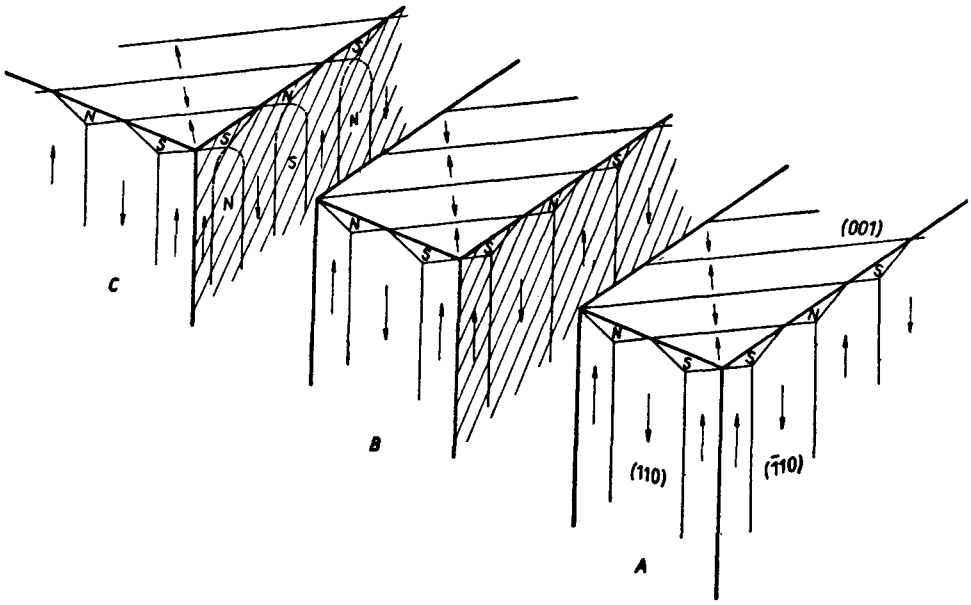

Fig. 7. Model of the *SL* domain structure (note the different crystallographic orientation of the crystal faces as compared with Fig. 3). The shaded cross-sections show that the 180° Bloch walls on the lateral crystal surfaces (110) and (1̄10) (as well as those on the surface (100) in Fig. 3) may either correspond to (180°|180°) Bloch walls inside the crystal (block *B*) or split into (90°|90°) Bloch walls (block *C*), as pointed out in [20]

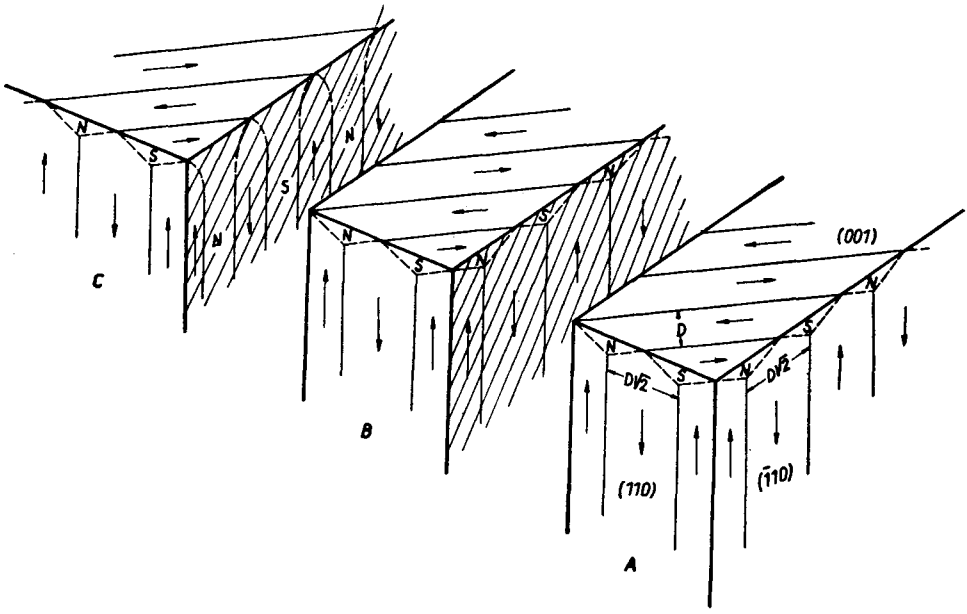

Fig. 8. Model of the modified Landau-Lifshitz (*ML*) domain structure corresponding to the powder patterns in Fig. 5 (*cp.* Fig. 2). For explanation of shaded cross-sections see Fig. 7

explanation of the powder patterns from Fig. 5 is by assuming the domain structure to be of the type shown schematically in Fig. 8, in which case however the "walls" between the closure domains and the main domains (marked by dashed lines in Figs 2 and 8) cannot be Bloch walls, as the normal component of the magnetization vector on passing through the wall changes. The fir-like secondary closure domains on the crystal surface (001)(see Fig. 5*a*, *c*) and the dagger-like closure domains shown in Fig. 5*e* arise because the crystal edges are rounded off in the process of polishing, as shown in the model in Fig. 9.

ACTA PHYSICA POLONICA Vol. XXXV (1969) Fasc. 5

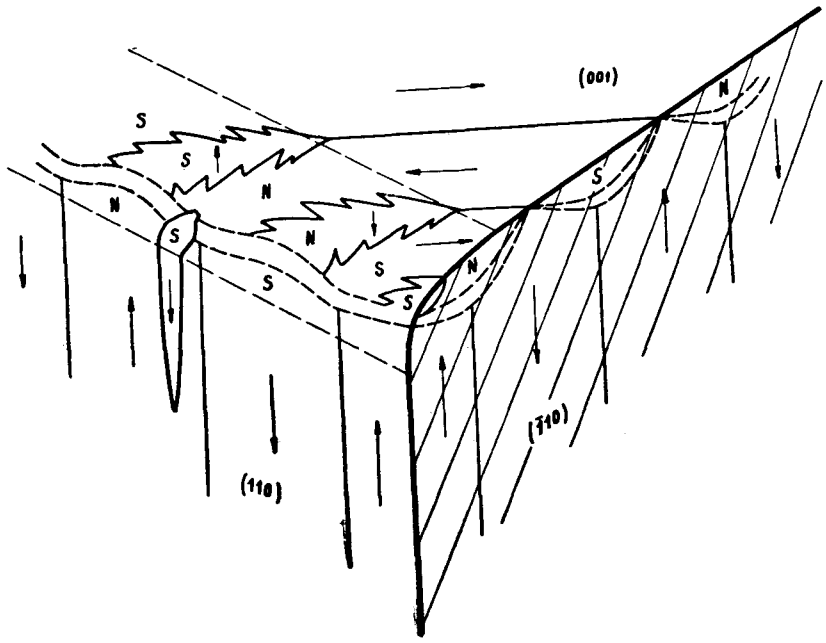

Fig. 9. Model of the *ML* domain structure (*cp.* block *B* in Fig. 8) with secondary (fir-like and dagger-like) closure domains at rounded-off crystal edges, as demonstrated in Fig. 5(*a*) and (*e*)

Because of its similarity to the *SL* domain structure, we shall call the structure from Fig. 8 the *modified* Landau–Lifshitz (*ML*) domain structure. To our knowledge, this domain structure is not yet known in the literature (see, *e.g.*, [15–17]).

We may note in passing that the 45°-inclination of the 180° Bloch walls towards the lateral crystal surfaces (110) contradicts the theoretical consclusions drawn in [18] (see also [16], *pp.* 288–300) according to which the angle of inclination should in our case be about 32°. Our experiment confirms instead the theoretical results obtained in [19] which predict 45°.

The results of our measurements are presented in Fig. 10 by the curves D_{SL} and D_{ML}, for the *SL* (Figs 1, 3, 4) and *ML* (Figs 2, 5, 8, 9) domain structures, respectively. The exponents b_m and the corresponding coefficients $a_{X;m}$ as defined in Eq. (2) are easily obtained from the diagram, *i.e.*,

$$b_1 = 0.5, \quad a_{SL;1} = 0.019 \text{ cm}^{0.5}, \quad a_{ML;1} = 0.03 \text{ cm}^{0.5} \tag{5}$$

a

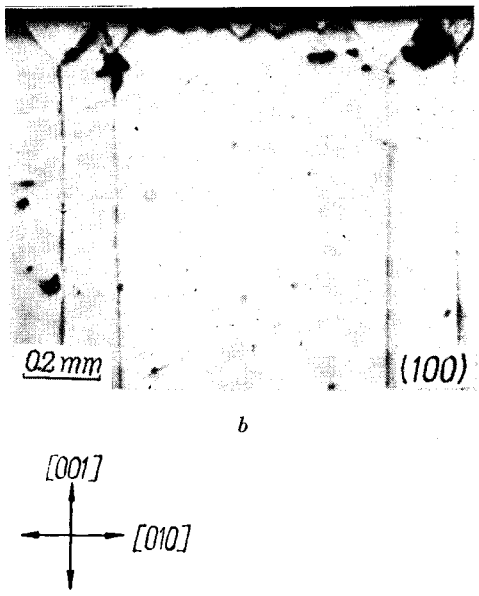

b

Fig. 4. Typical powder patterns from the lateral crystal surface (100) of the sample in Fig. 1 (*cp.* Fig. 3) Crystal thickness T in the direction [001]: (*a*) — 3 mm, (*b*) — 3.5 mm

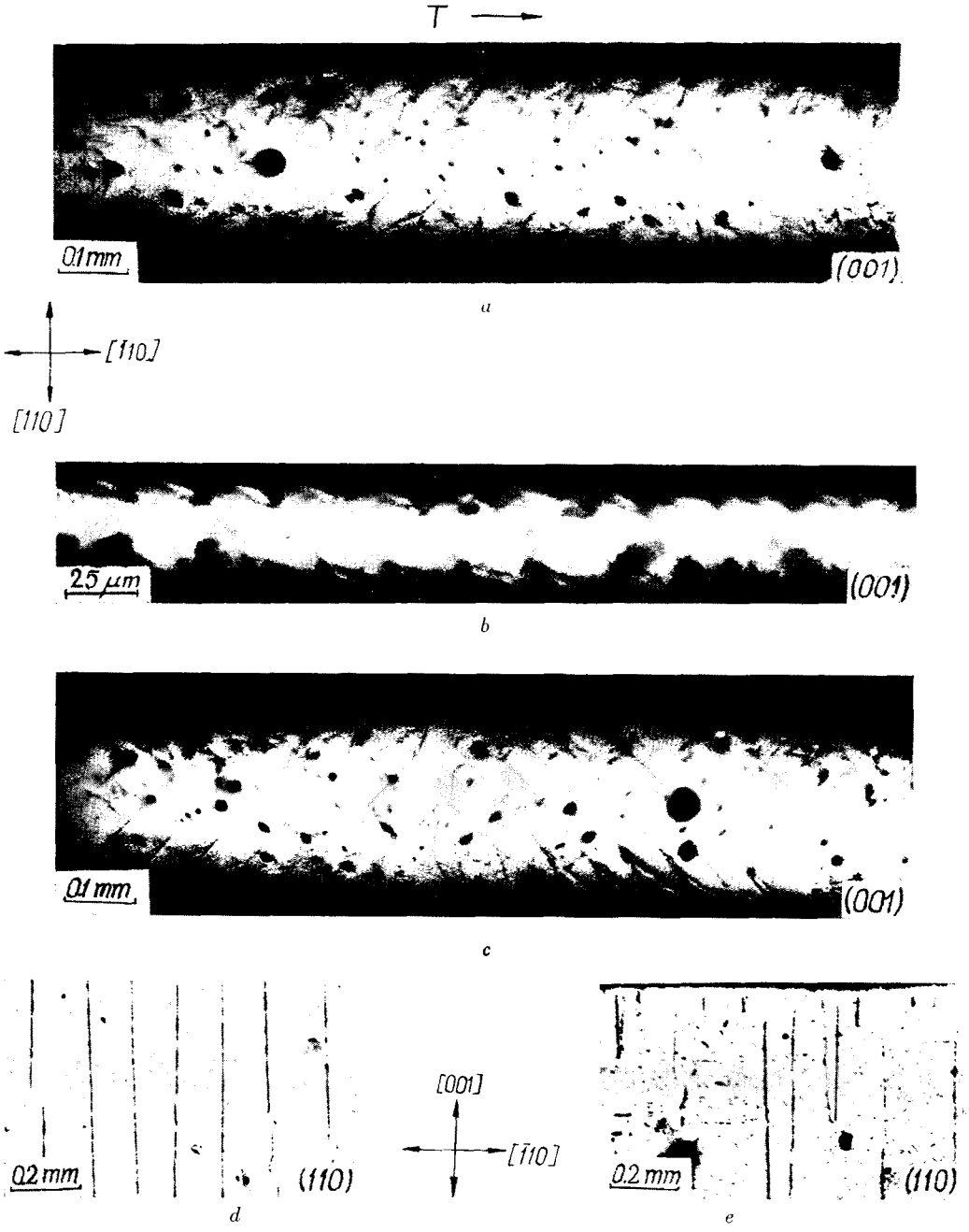

Fig. 5. Powder patterns from the upper surface (001) and the lateral surface (110) of the sample from Fig. 2, revealing the modified Landau Lifshitz (*ML*) domain structure (*cp.* models in Figs 8 and 9). Crystal thickness T in the direction [001] (at centres of photographs): (a) — 300 μm, (b) — 50 μm, (c) — 300 μm, (*d*) — 750 μm, (*e*) — 800 μm

for $T \leqslant T_0$, and

$$b_2 = 0.9, \quad a_{SL;2} = 0.068 \text{ cm}^{0.1}, \quad a_{ML;2} = 0.11 \text{ cm}^{0.1} \tag{6}$$

for $T \geqslant T_0$ (*cp.* Footnote 2). The critical thickness T_0 can be obtained either directly from the diagram or from the obvious relation

$$a_{X;1} T_0^{b_1} = a_{X;2} T_0^{b_2} \equiv D_X^0 \tag{7}$$

that interlocks T_0 with the quantities (5), (6). Hence, for Fe–3.25% Si we have

$$T_0 = (a_{X;1}/a_{X;2})^{\frac{1}{b_2 - b_1}} \cong 400 \ \mu\text{m} \equiv T_0^{FeSi}, \tag{8}$$

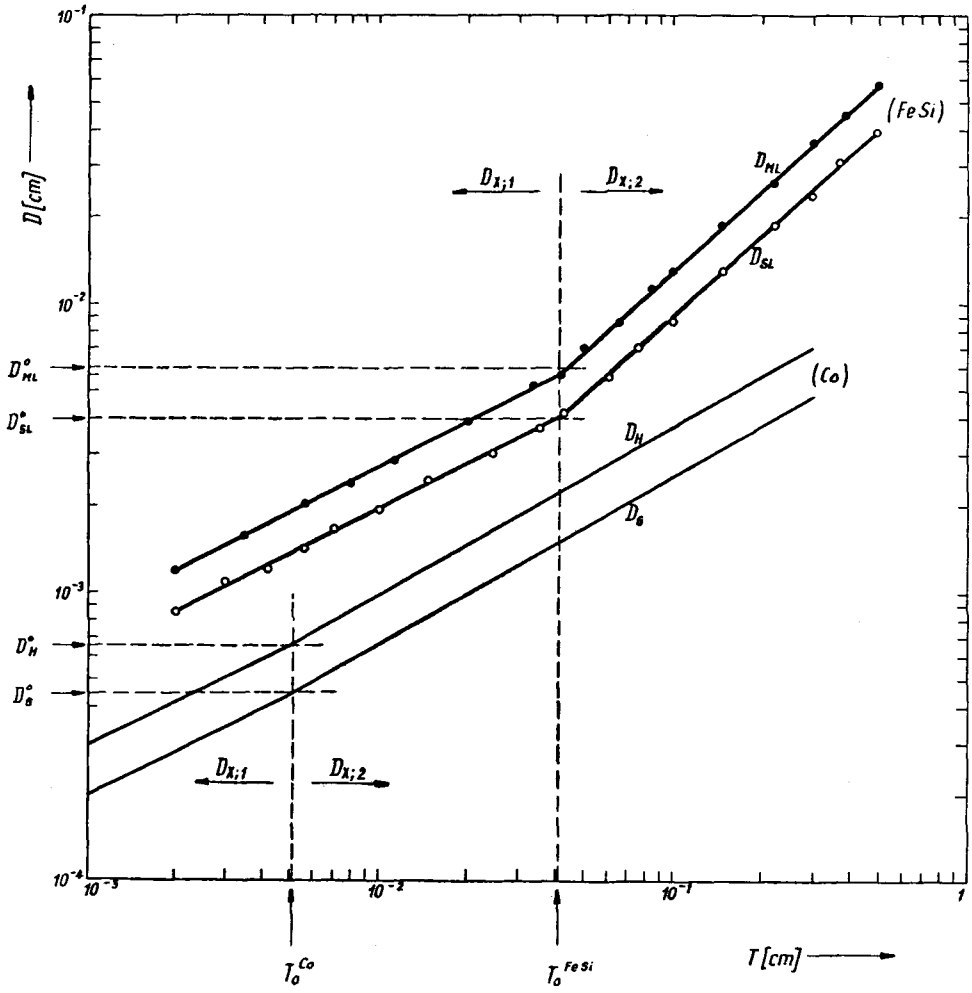

Fig. 10. Experimental curves showing the thickness dependence of the domain width, $D(T)$, for the simple (D_{SL}) and the modified (D_{ML}) Landau-Lifshitz domain structures in Fe—3.25% Si. The critical crystal thickness is $T_0 \cong 400 \ \mu\text{m} \equiv T_0^{\text{FeSi}}$, and the corresponding critical domain widths are $D^0_{SL} = 38 \ \mu\text{m}$ and $D^0_{ML} = 60 \ \mu\text{m}$, respectively. For comparison, the curves obtained in [1, 2] for the honeycomb (D_H) and the Goodenough (D_G) remanent domain structures in cobalt are shown. (Note the definition of D_{ML} in Fig. 8)

ACTA PHYSICA POLONICA Vol. XXXV (1969) Fasc. 5

and for the critical domain widths D_X^0 defined by (7) we obtain

$$D_X^0 \equiv D_{X;m}(T_0) = (a_{X;1}^{b_2}/a_{X;2}^{b_1})^{\frac{1}{b_2-b_1}},$$

$$D_{SL}^0 \cong 38\ \mu\text{m}, \qquad D_{ML}^0 \cong 60\ \mu\text{m}, \tag{9}$$

From (5)–(7) it follows that[3]

$$a_{SL;1}/a_{SL;2} = a_{ML;1}/a_{ML;2} = T_0^{0.4} \cong 0.28\ \text{cm}^{0.4},$$

$$a_{ML;1}/a_{SL;1} = a_{ML;2}/a_{SL;2} = D_{ML}^0/D_{SL}^0 \cong 1.6 \tag{10}$$

which confirms the general rule (4). By inserting the values (5) and (6) into (2) we have for Fe–3.25% Si the thickness dependence

$$D_{SL} = \begin{cases} D_{SL;1} = 0.019\ T^{0.5}\ [\text{cm}] & \text{for } T \leqslant T_0 \\ D_{SL;2} = 0.068\ T^{0.9}\ [\text{cm}] & \text{for } T \geqslant T_0 \end{cases} \tag{11}$$

for the *SL* domain structure, and

$$D_{ML} = \begin{cases} D_{ML;1} = 0.03\ T^{0.5}\ [\text{cm}] & \text{for } T \leqslant T_0 \\ D_{ML;2} = 0.11\ T^{0.9}\ [\text{cm}] & \text{for } T \geqslant T_0 \end{cases} \tag{12}$$

for the *ML* domain structure, where T and D are to be measured in cm and $T_0 = T_0^{FeSi} \cong 400\ \mu$m.

For comparison, the curves D_H and D_G obtained in [1–3] for the honeycomb (*H*) and the Goodenough (*G*) remanent domain structures in Co are given in Fig. 10.

3. *Theoretical considerations*

To examine the relationship between the critical crystal thickness T_0 and the domain srtucture energy, let us consider a simple energetic model of the *ML* structure from Fig. 8 in a rectangular-prism-shaped single crystal with thickness T, width W, and length L in the direction [001], [110], and [$\bar{1}$10], respectively. For the energy E_B of a single 180° Bloch wall with dimensions $T-pD$ and $W\sqrt{2}$ in the directions [001] and [100] we have

$$E_B = \gamma(T-pD)W\sqrt{2} \tag{13}$$

where γ is the energy density (per surface area) of the Bloch wall, D is the domain width, and $p > 0$ is an undetermined dimensionless parameter that accounts for the fact that the 180° Bloch walls do not reach the (001) crystal surfaces (*cp.* Fig. 9).

On the other hand, the interdomain regions between the primary closure domains at the (001) crystal surfaces and the main domains in the interior (marked by dashed lines

[3] Note that Eq. (7) implies $a_{X;1}/a_{X;2} = T_0^{b_2-b_1}$, $a_{X;m}/a_{Y;m} = D_X^0/D_Y^0$ which, in turn, determines the constants in Eq. (4).

in Fig. 9) represent another type of anisotropy energy which we shall denote by E_I (per Bloch wall) and assume in the form

$$E_I = qKWD^r \tag{14}$$

where K is the anisotropy constant. The coefficient $q > 0$ and the exponent r are to be determined from experiment. In this approximation, we neglect the magnetostatic self-energy arising from the magnetic poles at the crystal edges (*cp.* Fig. 9).

There are $L/D\sqrt{2}$ domains in the crystal. Thus, the total anisotropy energy E of the *ML* domain structure is

$$E = (E_B + E_I)L/D\sqrt{2} \tag{15}$$

and its density $\mathcal{E}$ per surface area in the plane (001) reads

$$\mathcal{E} \equiv E/LW = \gamma(T/D - p) + qKD^{r-1}/\sqrt{2}. \tag{16}$$

The minimum condition $\partial\mathcal{E}/\partial D = 0$ leads to

$$D = aT^b, \quad b = \frac{1}{r},$$

$$a = [b\gamma\sqrt{2}/qK(1-b)]^b, \quad q = \gamma\sqrt{2}/(r-1)a^rK. \tag{17}$$

Denoting $r_m \equiv 1/b_m$, $a_{ML;m} \equiv a_m$, $q_m \equiv q(r_m, a_m)$ and assuming $K = 3\times10^5$ erg/cm^3, $\gamma = 3.2$ erg/cm^2 we obtain from (5), (6) and (17)

$$\begin{aligned} &r_1 = 0.5,\ q_1 = 0.017 && \text{for } T \leqslant T_0, \\ &r_2 = 1.1,\ q_2 = 1.7\times10^{-3}\ \text{cm}^{0.9} && \text{for } T \geqslant T_0 \end{aligned} \tag{18}$$

with T_0 from Eq. (8).

Upon inserting the solution (17) into (13)–(16) we have for the minimum energies

$$\begin{aligned} \mathcal{E}_B^0 &\equiv E_B^0/LW = \gamma(T^{1-b}/a - p), \\ \mathcal{E}_I^0 &\equiv E_I^0/LW = \gamma b T^{1-b}/a(1-b), \\ \mathcal{E}^0 &= \gamma[T^{1-b}/a(1-b) - p], \\ \mathcal{E}_I^0/\mathcal{E}_B^0 &= b/(1-b)(1-paT^{b-1}) \equiv P. \end{aligned} \tag{19}$$

With $b = b_1 = 0.5$, $a = a_1 = 0.03$ cm$^{0.5}$ for $T \leqslant T_0$ and $b = b_2 = 0.9$, $a = a_2 = 0.11$ cm$^{0.1}$ for $T \geqslant T_0$ one obtains

$$\begin{aligned} &\mathcal{E}_B^0 = (107 \cdot T^{0.5} - 3.2p)\ \text{erg/cm}^2, \quad \mathcal{E}_I^0 = 107 \cdot T^{0.5}\ \text{erg/cm}^2, \\ &\mathcal{E}^0 = (214 \cdot T^{0.5} - 3.2p)\ \text{erg/cm}^2, \quad P = (1 - 0.03\,p/T^{0.5})^{-1} \end{aligned} \tag{20}$$

ACTA PHYSICA POLONICA Vol. XXXV (1969) Fasc. 5

ACTA PHYSICA POLONICA Vol. XXXV (1969) Fasc. 5

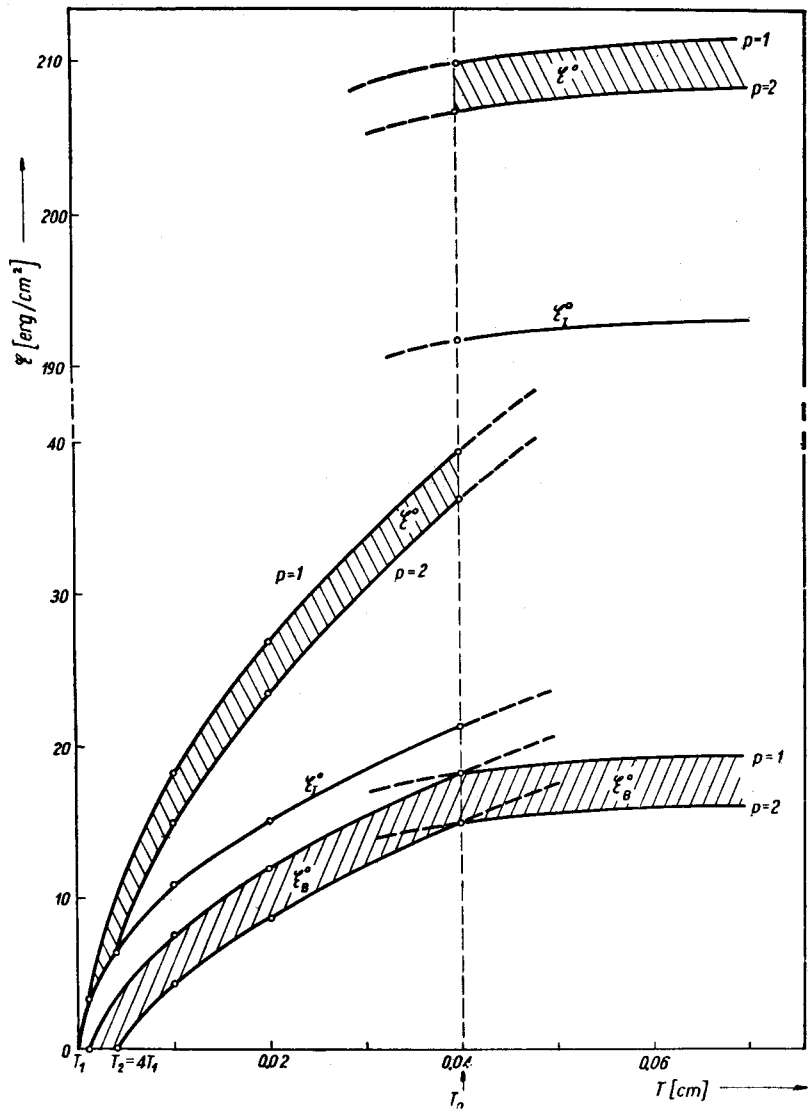

Fig. 11. Curves of the energies $\mathcal{E}_B^0$, $\mathcal{E}_I^0$ and $\mathcal{E}^0$ given by Eqs. (20), (21) and corresponding to the *ML* domain structure from Fig. 8

for $T \leqslant T_0$, and

$$\mathcal{E}_B^0 = (29.1 \cdot T^{0.1} - 3.2\,p)\ \mathrm{erg/cm^2}, \qquad \mathcal{E}_I^0 = 262 \cdot T^{0.1}\ \mathrm{erg/cm^2},$$

$$\mathcal{E}^0 = (291 \cdot T^{0.1} - 3.2\,p)\ \mathrm{erg/cm^2}, \qquad P = 9/(1 - 0.11\,p/T^{0.1}) \tag{21}$$

for $T \geqslant T_0$, where T is to be measured in cm.

The dependence of the energies (20), (21) on the crystal thickness T is illustrated in Fig. 11 for two values of the parameter p. It is seen that $\mathcal{E}_I^0$ has a discontinuity at T_0. The energy jump $\Delta\mathcal{E}_I^0$ is easily calculated from (19)–(21) by utilizing the formulae (7)–(9):

$$\Delta\mathcal{E}_I^0 = \lim_{T\to T_0+0} \mathcal{E}_I^0 - \lim_{T\to T_0-0} \mathcal{E}_I^0 \tag{22}$$

$$= (a_1^{1-b_2}/a_2^{1-b_1})^{\frac{1}{b_2-b_1}}(b_2-b_1)/(1-b_1)(1-b_2) \cong 170.4\ \mathrm{erg/cm^2}.$$

This discontinuity does not depend on p and manifests itself in the total energy $\mathcal{E}^0$. Note that for $p = 0$

$$\mathcal{E}_I^0 = \mathcal{E}_B^0 \quad \text{for } T \leqslant T_0,$$

$$\mathcal{E}_I^0 = 9\mathcal{E}_B^0 \quad \text{for } T \geqslant T_0. \tag{23}$$

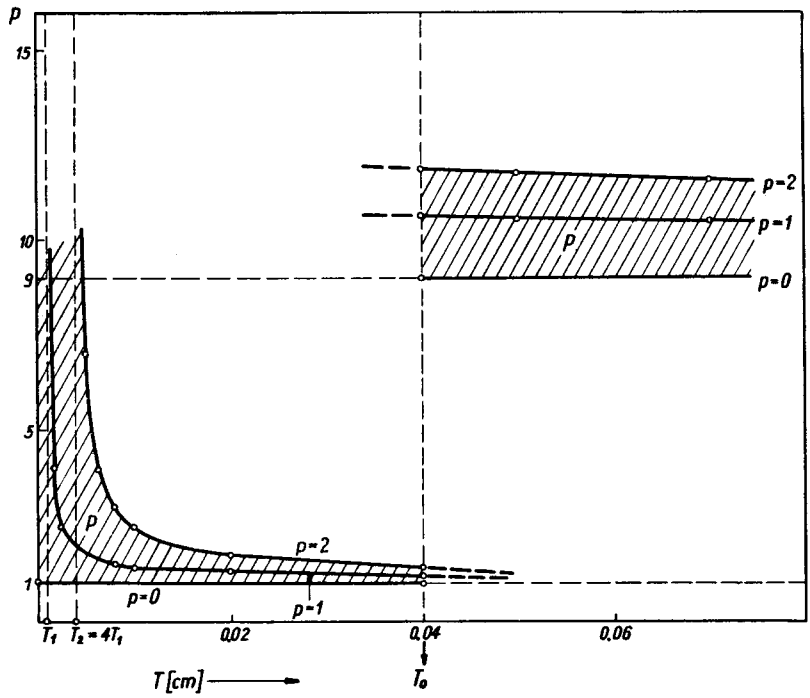

Fig. 12. Curves of the ratio $P = \mathcal{E}_I^0/\mathcal{E}_B^0$ for $p = 0, 1, 2$ (*cp.* Fig. 11)

The relative contributions of the energies $\mathcal{E}_B^0$ and $\mathcal{E}_I^0$ to the total energy $\mathcal{E}^0$ is illustrated in Fig. 12, where the ratio $P = \mathcal{E}_I^0/\mathcal{E}_B^0$ is plotted as a function of T, for $p = 0, 1, 2$. Note that for $0 < p < T/D$

$$\lim_{T\to\infty} P(T) = 9, \quad \lim_{T\to T_p+0} P(T) = \infty \tag{24}$$

ACTA PHYSICA POLONICA Vol. XXXV (1969) Fasc. 5

where T_p is defined by the equation

$$\mathcal{E}_B^0(T_p) = 0,$$

$$T_p = (pa_1)^{\frac{1}{1-b_1}} = \begin{cases} 0 \\ T_1 = 9\ \mu\text{m} \\ T_2 = 4\,T_1 \end{cases} \quad \text{for} \quad \begin{cases} p = 0 \\ p = 1 \\ \text{p} = 2 \end{cases} \tag{25}$$

One easily verifies that sign $\mathcal{E}_B^0(T) = \text{sign}\,(T - T_p)$.

To prove the stability of the *ML* domain structure described by the energy (15), we calculate from (16)

$$\frac{\partial^2 \mathcal{E}}{\partial D^2} = D^{-3}\{2\gamma T + qKD^r(r-2)\,(r-1)/\sqrt{2} \equiv \Delta(T) \tag{26}$$

and insert the solution (17), which leads to

$$\Delta = r\gamma T/D^3 > 0 \tag{27}$$

as $r > 0$ according to (18).

4. *Concluding remarks*

The experimental results obtained in the present paper for the *SL* and *ML* domain structures in Fe–3.25%Si provide further evidence that the thickness dependence of the domain width as given by formula (2) is by no means restricted to remanent domain structures or uniaxial ferromagnets, and may well apply to any regular domain structure in any ferromagnetic (or ferrimagnetic, for that matter) material. The same is probably true for the rules(4) or, equivalently, for the continuity condition (7) (see also Footnote 3). Table I summarizes the results presented here and in [1–3]. Although our conclusions are based on results obtained with four different regular domain structures and two different ferromagnetic materials (uniaxial Co and three-axial FeSi), it is clear that analogous experiments on a four-axial ferromagnetic material, such as Ni, are needed in proving the general validity of formulae (2) and (4). This is deferred to future investigations.

We would like to emphasize that, unlike in Co where the critical thickness T_0 can be identified as the thickness below which the dagger-like closure domains at the basal crystal surface disappear, there is no such simple interpretation of T_0 in the present case, as neither in the *SL* nor in the *ML* domain structure did the powder patterns on the (001) crystal surface show any significant changes below or above T_0. From this point of view there seems to be no obvious explanation of the sharp (and much more pronounced than in Co) increase of the D_{SL} and D_{ML} curves at T_0, Fig. 10. This indicates that the symmetry of the nternal domain structure must apparently change at T_0 which, *e.g.*, would account for the energy discontinuity shown in Fig. 11.

As seen from the solution (17), an energy term of the form (14) when added to the Bloch wall energy (13) leads to the correct type of thickness dependence of the domain width. It seems hopeless however, to try to derive it (or an equivalent expression) from theory, so

ACTA PHYSICA POLONICA Vol. XXXV (1969) Fasc. 5

TABLE I

Material		Fe — 3.25% Si				Co			
Critical crystal-thickness T_0		400 μm				50 μm			
Domain structure		Landau-Lifshitz				Honeycomb		Goodenough	
		Standard		Modified					
Symbol X		SL		ML		H		G	
Crystal thickness T		$T \leqslant T_0$	$T \geqslant T_0$	$T \leqslant T_0$	$T \geqslant T_0$	$T < T_0$	$T > T_0$	$T < T_0$	$T > T_0$
Exponent b_m	b_1	0.5	—	0.5	—	0.5	—	0.5	—
	b_2	—	0.9	—	0.9	—	0.57	—	0.57
Coefficient $a_{X;m}[\mathrm{cm}^{1-b_m}]$	$a_{X;1}[\mathrm{cm}^{1-b_1}]$	0.019 $\mathrm{cm}^{0.5}$	—	0.030 $\mathrm{cm}^{0.5}$	—	0.010 $\mathrm{cm}^{0.5}$	—	0.007 $\mathrm{cm}^{0.5}$	—
	$a_{X;2}[\mathrm{cm}^{1-b_2}]$	—	0.068 $\mathrm{cm}^{0.1}$	—	0.110 $\mathrm{cm}^{0.1}$	—	0.015 $\mathrm{cm}^{0.43}$	—	0.010$\mathrm{cm}^{0.43}$
Critical domain width $D_X^0 \equiv D_X(T_0) = a_{X;m} T_0^{b_m}$		38 μm		60 μm		6.6 μm		4.5 μm	
$a_{X;1}/a_{X;2} = T_0^{b_2-b_1}$ $[\mathrm{cm}^{b_2-b_1}]$		0.28 $\mathrm{cm}^{0.4}$				0.68 $\mathrm{cm}^{0.07}$			
$a_{X;m}/a_{Y;m} = D_X^0/D_Y^0$		$a_{ML;m}/a_{SL;m} \cong 1.6$				$a_{H;m}/a_{G;m} \cong 1.5$			

as to be able to calculate q and r instead of determining their values from experimental results. For this reason, the results of the theoretical considerations in Sec. 3 are mainly these that T_0 is shown to be connected with an energy discontinuity, and that beside the Bloch wall energy E_B an energy term of the type (14) is needed if a thickness dependence of the form (17) is to follow from theory. It is to be noted that, in the case of the *SL* domain structure, this speaks in favour of the existence of (90°|90°) Bloch walls inside the crystal as suggested in [20] (*cp.* Fig. 3 and block *C* in Fig. 7). Otherwise there are no interdomain regions whatever which would justify an energy term of the type (14) with $r > 1$. (Note that the (90°|180°) Bloch walls between the closure domains and the main domains in Fig. 3 lead to an energy term which is linear with respect to D, and that this term when added to E_B from Eq. (13) leads upon minimization to the trivial result $D = \infty$.)

ACTA PHYSICA POLONICA Vol. XXXV (1969) Fasc. 5

REFERENCES

[1] B. Wysłocki, *Acta Phys. Polon.*, **34,** 327 (1968).
[2] B. Wysłocki, *Acta Phys. Polon.*, **35,** 179 (1969).
[3] B. Wysłocki and W. J. Ziętek, *Acta Phys. Polon.*, **35,** 117 (1969).
[4] H. J. Williams, R. M. Bozorth and W. Shockley, *Phys. Rev.*, **75,** 155 (1949).
[5] D. Bloor and D. H. Martin, *Proc. Phys. Soc.*, **73,** 694 (1959).
[6] R. Carey, *Proc. Phys. Soc.*, **74,** 567 (1960).
[7] C. G. Dunn and G. C. Nonken, *Metall Progress*, **64,** 71 (1953).
[8] G. Sołtysik and B. Wysłocki, *Prace Instytutów Hutniczych*, **19,** 247 (1967) (in Polish — with abstracts in English and Russian).
[9] W. C. Elmore, *Phys. Rev.*, **51,** 982 (1937); **53,** 757 (1938).
[10] J. R. Garrood, *Proc. Phys. Soc.*, A **79,** 1252 (1962).
[11] B. Wysłocki and J. W. Ziętek, *Acta Phys. Polon.*, **21,** 433 (1962).
[12] B. Wysłocki and W. J. Ziętek, *Postępy Fizyki*, **14,** 307 (1963) (in Polish).
[13] B. Wysłocki and W. J. Ziętek, *Acta Phys. Polon.*, **29,** 223 (1966).
[14] L. D. Landau and E. Lifshitz, *Phys. Z. Sov.*, **8,** 153 (1935).
[15] D. J. Craik and R. S. Tebble, *Ferromagnetism and Ferromagnetic Domains*, North-Holland Publ. Co., Amsterdam 1965.
[16] A. Seeger (editor), *Chemische Bindung in Kristallen und Ferromagnetismus*, Springer-Verlag, Berlin — New York 1966.
[17] R. Carey and E. D. Isaac, *Magnetic Domains and Techniques for their Observation*, The English University Press. London 1966.
[18] C. D. Graham and P. W. Neurath, *J. Appl. Phys.*, **28,** 888 (1957).
[19] M. Matlak and A. Wachniewski, *Acta Phys. Polon.*, **32,** 959 (1967).
[20] W. J. Ziętek, *Acta Phys. Polon.*, **32,** 385 (1967).